Carbon isotope compositions of terrestrial C3 plants as indicators of (paleo)ecology and (paleo)climate

Matthew J. Kohn[1]

Department of Geosciences, Boise State University, Boise, ID 83725

Edited by Mark H. Thiemens, University of California, San Diego, La Jolla, CA, and approved September 24, 2010 (received for review April 11, 2010)

A broad compilation of modern carbon isotope compositions in all C3 plant types shows a monotonic increase in $\delta^{13}C$ with decreasing mean annual precipitation (MAP) that differs from previous models. Corrections for temperature, altitude, or latitude are smaller than previously estimated. As corrected for altitude, latitude, and the $\delta^{13}C$ of atmospheric CO_2, these data permit refined interpretation of MAP, paleodiet, and paleoecology of ecosystems dominated by C3 plants, either prior to 7–8 million years ago (Ma), or more recently at mid- to high latitudes. Twenty-nine published paleontological studies suggest preservational or scientific bias toward dry ecosystems, although wet ecosystems are also represented. Unambiguous isotopic evidence for C4 plants is lacking prior to 7–8 Ma, and hominid ecosystems at 4.4 Ma show no isotopic evidence for dense forests. Consideration of global plant biomass indicates that average $\delta^{13}C$ of C3 plants is commonly overestimated by approximately 2‰.

aridity | carbon cycle | closed canopy | paleoprecipitation

Plants exhibiting C3 photosynthesis have dominated the history of terrestrial vegetation, as CAM plants occupy only a small percentage of typical ecosystems (e.g., 1), and C4 plants became abundant in grasslands only within the last 7–8 million years (2). C3 plants exhibit a large range of carbon isotope compositions (−20 to −37‰, V-PDB; Fig. 1), generally reflecting a physiological response to aridity (anomalously high $\delta^{13}C$) and a combination of low light levels plus leaf litter recycling (anomalously low $\delta^{13}C$; 3). Past studies have conflicted on the dependence of $\delta^{13}C$ on mean annual precipitation (MAP). Most studies support a negative correlation (e.g., 4), but some have reported no correlation (5) or even a positive correlation (6).

This study explores carbon isotope systematics of C3 plants through a comprehensive compilation of literature data, minimizing local differences that have given rise to disparate interpretations. This work directly benefits paleodietary and paleoecological studies by providing estimates of MAP in ancient environments as well as clearer boundaries for identifying the understory of closed-canopy forests and the contribution of non-C3 plants to diet, which is used to gain insights into C4 origins (2). The new compilation also helps refine models of the modern carbon cycle by providing a better estimate of global C3 $\delta^{13}C$ values (7). The present analysis differs from a recent investigation of correlations between tree + shrub $\delta^{13}C$ and MAP or plant functional type (8) in that it is several times larger on a site-by-site basis, spans the full range of plant growth forms (including trees, bushes, grasses, and herbs), averages data from each site to minimize sampling bias (4), and regresses an arguably more appropriate function to the data. Selection criteria of climate and isotopic data also differ slightly. This broader approach of considering all C3 plants and averaging compositions is important when evaluating herbivore paleodiets, which are not restricted to trees, and further reveals significant differences in modeled compositions at low MAP and in the estimated effect of altitude and latitude. A simple function allows MAP to be estimated from $\delta^{13}C$ of fossil bone collagen and tooth enamel and used for inferring terrestrial climate change. Past studies of dietary ecology and global C3 plant $\delta^{13}C$ values further indicate an analytical bias toward dry ecosystems.

Results

Data. The dataset, provided in Dataset S1, encompasses all types of C3 plants, including trees, shrubs, herbs, and grasses from approximately 570 individual sites, and spans ranges of MAP, mean annual temperature (MAT), altitude, and latitude of 1 to 3,700 mm/yr, −13.5 to 28.4 °C, −391 to 4,900 m, and 54.9°S to 69.5°N. This dataset is *ca.* six times larger than any previous analysis of C3 isotopic systematics and covers more types of C3 plants.

C3 Data Distributions. For the global C3 $\delta^{13}C$ dataset, a histogram of corresponding MAP values (Fig. 1*A*) demonstrates research bias toward dry ecosystems (high $\delta^{13}C$) and tropical rain forests (low $\delta^{13}C$). Thus the histogram of $\delta^{13}C$ values, which shows the well-known range from −20 to −37‰ (Fig. 1*B*), is broader than expected for global C3 biomass. Values above −23‰ are almost completely restricted to the Atacama Desert (9), the driest desert on Earth, and to *Pinus* in dry settings (10). Values below −31.5‰ reflect canopy effects in low-light tropical forests. The compilation from O'Leary (11; downward corrected by −0.25‰ for fossil fuel burning) and from this study average about −27.25‰ and −27.0‰, respectively, omitting understory analyses below −31.5‰.

Correlation of MAP with $\delta^{13}C$. Carbon isotope compositions exhibit a systematic change over the range of MAP, excepting low $\delta^{13}C$ values associated with the understory of dense forests (Figs. 1 and 2). High $\delta^{13}C$ values (above −25.5‰) are essentially restricted to environments with MAP < 500 mm/yr. The trend noticeably "flattens" at high MAP, indicating nearly constant isotopic discrimination in wet environments. Other attempts to quantify this correlation have resulted in widely disparate results (Fig. 2), largely because they were based on limited datasets. The results of Stewart et al. (4) and Diefendorf et al. (8) most closely match the new compilation, but the Stewart et al. model deviates from observations at MAP > 1,000 mm/yr, whereas the Diefendorf et al. model predicts unusually high $\delta^{13}C$ values at low MAP (Fig. 2). The preferred equation for MAP as a function of $\delta^{13}C$ is:

$$\begin{aligned}\delta^{13}C(‰,\text{VPDB}) = &-10.29 + 1.90\times10^{-4}\ \text{Altitude (m)}\\ &- 5.61\log_{10}(\text{MAP} + 300,\ \text{mm/yr})\\ &- 0.0124\ \text{Abs (latitude,°)}\end{aligned} \quad \textbf{[1]}$$

or alternatively for Δ:

Author contributions: M.J.K. designed research, performed research, contributed new reagents/analytic tools, analyzed data, and wrote the paper.

The author declares no conflict of interest.

This article is a PNAS Direct Submission.

[1]E-mail: mattkohn@boisestate.edu.

This article contains supporting information online at www.pnas.org/lookup/suppl/doi:10.1073/pnas.1004933107/-/DCSupplemental.

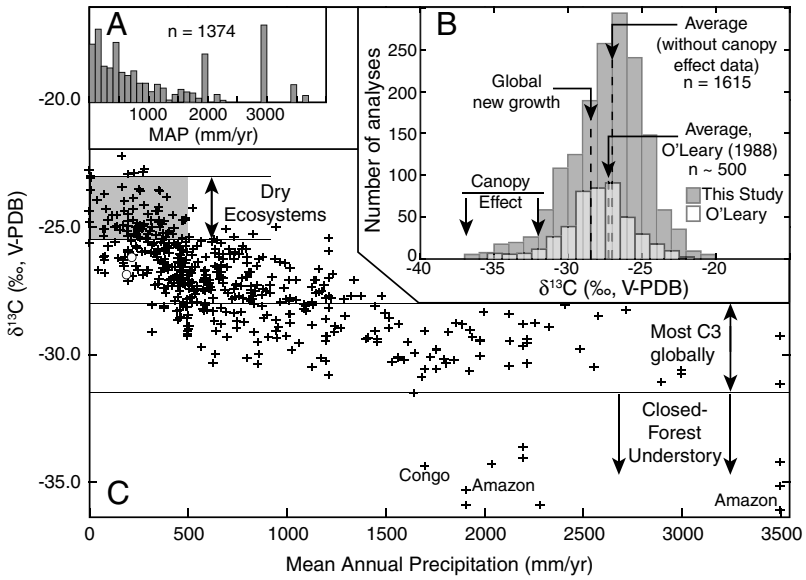

Fig. 1. (*A*) Histogram of MAP values for isotopically charact.erized C3 plants, showing emphasis on relatively arid ecosystems (MAP ≤ 500 mm/yr) and tropical rainforests (spikes at MAP ~ 2,000, 3,000 mm/yr). (*B*) Histogram of $\delta^{13}C$ values of modern C3 plants. Data compiled in this study average −27.0‰, excluding analyses from the understory of closed-canopy forests. Estimated global average composition, based on global trends in precipitation and vegetation, is approximately −28.5‰, significantly lower than typically assumed. An accurate average $\delta^{13}C$ value for C3 plants is needed for accurate models of carbon fluxes, atmospheric CO_2 compositions, and soil organic matter. (*C*) $\delta^{13}C$ values vs. MAP showing increasing $\delta^{13}C$ with aridity. Data sources are listed in *SI Text*. White dots are average compositions of data from a large collection made in a single month during a wet year (35).

$$\Delta(‰,\text{VPDB}) = 2.01 - 1.98\times10^{-4}\ \text{Altitude (m)} + 5.88\log_{10}(\text{MAP} + 300,\ \text{mm/yr}) + 0.0129\ \text{Abs (latitude,°)} \quad [2]$$

where:

$$\Delta = \frac{\delta^{13}C_{atm} - \delta^{13}C_{leaf}}{1 + \delta^{13}C_{leaf}/1000} \quad [3]$$

(3). Both regressions have an R^2 of 0.59, a significant improvement over the functional form used by Diefendorf et al. (8; R^2 = 0.34, including their altitude and latitude coefficients). These equations allow evaluation of the effects of MAP, altitude, and latitude on $\delta^{13}C$ values or Δ, or alternatively estimation of MAP from altitude, latitude, and $\delta^{13}C$ or Δ. Note that the altitude coefficient is smaller by a factor of 3 to 5,000 than indicated in other studies (8, 12). Latitudinal effects have not been estimated for data that simultaneously account for altitude and MAP. Uncertainties of ±0.5‰ in mean $\delta^{13}C$ or Δ propagate to uncertainties in MAP of as little as ±100 mm/yr at MAP = 100–500 mm/yr, to ±500 mm/yr at MAP ~ 2,000 mm/yr.

Discussion

Average C3 Composition and Isotopic Bounds on C3 $\delta^{13}C$. A commonly quoted "average" C3 composition ($\delta^{13}C_{C3,ave}$) is −26 to −27‰ (e.g., 2, 13–15) similar to or slightly higher than compilation means (Fig. 1). Such high values, however, are strongly biased toward dry ecosystems (Fig. 1*A*). For example, the global $\delta^{13}C_{C3,ave}$, as estimated from Eq. **3** and distributions of plant biomass and precipitation, is approximately −28.5‰, or approximately 2‰ lower than commonly assumed. This low $\delta^{13}C_{C3,ave}$ mainly reflects the importance of equatorial and midlatitude northern hemisphere C3 biomass, which is less well represented in the literature. The $\delta^{13}C_{C3,ave}$ value is important for models of carbon fluxes, atmospheric CO_2 compositions, and soil organic matter (e.g., 7, 15–17). Seasonal changes to $\delta^{13}C_{atm}$ depend on C3–C4 biomass ratios and their compositions, and differences in modeled C3 biomass discrimination perturb predicted $\delta^{13}C$ of atmospheric CO_2 most strongly (16). The dataset and equations developed here could be used to test and calibrate these models. Considering that $\delta^{13}C > -23‰$ is restricted to MAP < 10 mm/yr, non-C3 vegetation (e.g., C4 plants, lichen, or CAM plants) or the genus *Pinus* in some settings, this value is recommended as a likely maximum for typical C3 plants. Likewise, $\delta^{13}C < -31.5$ is recommended as a cutoff indicating the understory of closed-canopy forests.

Paleoprecipitation Reconstructions. The regressed curve allows prediction of MAP from the average modern equivalent of diet composition ($\delta^{13}C_{diet,meq}$), which can be estimated from fossil tooth or collagen $\delta^{13}C$ values and $\delta^{13}C_{atm}$ (see *SI Text*). Most studies that inferred mixed C3-C4 ecosystems were omitted from consideration because obvious C4 consumption ($\delta^{13}C_{diet,meq}$ values for individual species well above −22‰) would otherwise imply low or negative MAP. Corrections for $\delta^{13}C_{atm}$ are key for predicting accurate C3 composition and MAP. For example, two high values for tooth enamel $\delta^{13}C$ at approximately 15.5 Ma in East Africa (c. −8‰; 18) were interpreted as approximately 2‰ higher than the range of C3 compositions, requiring a C4 dietary component. A high $\delta^{13}C_{atm}$ at that time (c. −5.25, or a 2.75‰ downward correction), however, implies $\delta^{13}C_{diet,meq}$ of ~ − 24.8‰, well within the range of a pure C3 diet in dry ecosystems (Fig. 1*B* and Fig. 3, "*m*1"). Similarly large corrections apply to several other studies (19–21) and indicate wetter conditions than suggested by corrections for modern fossil fuel burning alone (c. −1.5‰ correction).

Results correlate generally with previous interpretations regarding "dry" vs. "wet" environments and with the possibility of alternative food sources. Few independent measures of MAP are available but include estimates of 300–700 mm/yr for late Cenozoic Spain (22) vs. ~500 mm/yr (Fig. 3, "*v*"), approximately 1,200 mm/yr for Paleocene-Eocene strata in Wyoming (23) vs. ~1,000 mm/yr (Fig. 3, "*k*"), and 740 ± 280 mm/yr for Eocene-Oligocene strata in Nebraska (24) vs. approximately 200 mm/yr (Fig. 3, "*z*"). In the latter case, only a few taxa were analyzed, probably compromising estimates of average compositions. Several

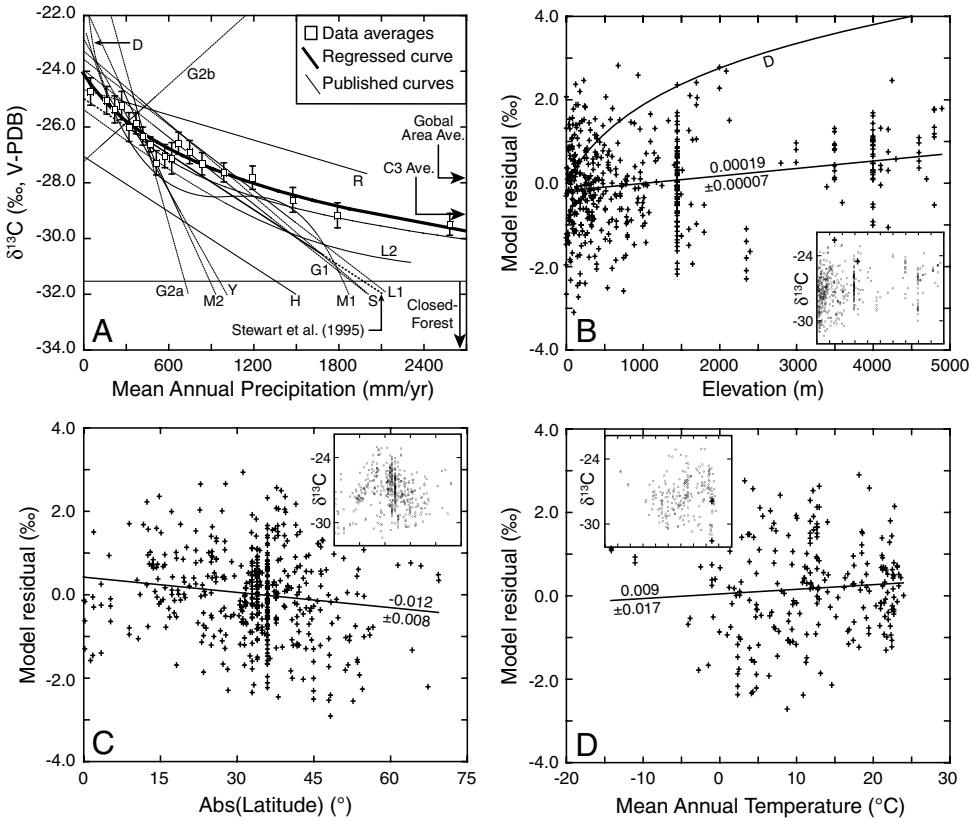

Fig. 2. (*A*) Averaged δ^{13}C (Table S1) vs. MAP and models of carbon isotope compositions. Averaged data are provided for clarity; thin lines are published models; thick curve is preferred regression from this study. Solid portions of lines represent MAP range over which models were developed; dotted lines show extrapolations. *D* = Diefendorf et al. (8); *G*1 = Gouveia and Freitas (54); *G2a,b* = Guo and Xie (6); *H* = Hatté et al. (55); *L*1 = Leffler and Enquist (56); *L*2 = Liu et al. (57); *M*1 = Miller et al. (58); *M*2 = Macfarlane et al. (59); *R* = Roden et al. (60, averaged from two similar regressions); *S* = Song et al. (61); *Y* = Youfeng et al. (62). Original line of Stewart et al. (4) is best linear model, but deviates from data at large values of MAP; model of Diefendorf et al. (8) fits high MAP data but does not predict low MAP data well. (*B*) Carbon isotope residuals for a model that omits latitude and altitude, showing significant correlation with altitude. "*D*" indicates model of Diefendorf et al. (8). Inset shows raw δ^{13}C values (uncorrected for any parameter) vs. altitude. (*C*) Carbon isotope residuals for a model that includes altitude but omits latitude, showing small but significant correlation. Inset shows raw δ^{13}C values (uncorrected for any parameter) vs. latitude; high values centered at approximately 30° latitude reflect dry ecosystems on Earth. (*D*) Carbon isotope residuals for a model that includes latitude and altitude vs. MAT showing no significant trend. Inset shows raw δ^{13}C values (uncorrected for any parameter) vs. MAT. Numbers are values for slopes, and errors are $\pm 2\sigma$. X-axes on insets are same as in encompassing panel.

other paleoenvironments were viewed as particularly wet, either from paleobotanical and paleofaunal observations or because of geographic location (20, 21, 25, 26). For three of these studies, estimates of average MAP for these localities exceed 2,000 mm/yr. For data from the Eocene Arctic (21), the relatively high δ^{13}C value results from the latitude correction, and a smaller correction would result in a higher estimated MAP. Only two studies have reported sufficiently low δ^{13}C for any fossil species to indicate closed-canopy conditions (20, 27). Taxonomically extensive isotopic data do not directly support the conclusion that the early hominid *Ardipithecus ramidus* occupied a closed forest (28); the lowest inferred $\delta^{13}C_{diet,meq}$ is approximately $-30.5‰$ (for a colobine monkey), and the assumed isotopic boundary for closed-canopy forests $\delta^{13}C_{diet,meq} = -27.8‰$) was unrealistically high. Overall most data from most studies appear to support low MAP, typically <800 mm/yr, below mean global MAP between 60°S and 75°N (~850 mm/yr). This probably reflects overall preservation or research bias toward drier ecosystems.

Two studies indicated average $\delta^{13}C_{diet,meq}$ above the range of average C3 δ^{13}C. Wang et al. (29) inferred consumption of high δ^{13}C C4 plants, which is consistent with the new compilation (Fig. 3, "*w*") and with individual $\delta\delta^{13}C_{diet,meq}$ values for several taxa above $-22‰$ (i.e., generally inaccessible to C3 plants). Pleistocene Irish deer data imply either dietary specialization on high $\delta^{13}C_{diet,meq}$ C3 plants (Fig. 3, point "*c*1"; 30), or lichen consumption (31).

Several qualifications apply to estimating MAP. First, environments with C4 plants cannot be interpreted because high $\delta^{13}C_{diet,meq}$ may reflect C4 consumption rather than aridity, although closed-canopy occupancy or C4 consumption can be evaluated. Second, C3 plant isotope compositions within a single locality show significant variation (e.g., Fig. 1*B*), and different taxa prefer different microhabitats and foods. Robust estimates of MAP thus require averaging over multiple taxa in a single locality, just as strong correlations between global plant δ^{13}C and MAP require averaging (4; this study). Some studies analyze numerous taxa (27, 32) and are well suited for estimating MAP, whereas others focus on specific ecological or climatic questions with only a few taxa or even just one taxon (19, 30, 33, 34), and MAP estimates are more tentative. Dry environments may contain wet microhabitats, e.g., along rivers or at springs, and flora may exhibit relatively low δ^{13}C values either seasonally or in an unusually wet year. For example, δ^{13}C of plants from the dry environments in one study (35) might be interpreted as higher MAP. In the most arid environments, plants may preferentially grow in cracks or declivities where precipitation accumulates, effectively increasing MAP (36), and other sources of precipitation, such as fog, may contribute significantly to total moisture (37, 38). These processes provide greater moisture than implied by MAP alone, and in these cases paleo-MAP estimates will be

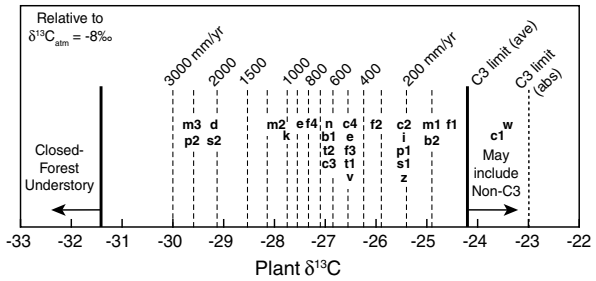

Fig. 3. Paleodietary compositions corrected for altitude and latitude contoured for MAP; this plot permits interpretation of paleoenvironments from carbon isotope compositions of fossil tooth enamel or collagen. Tooth enamel and collagen compositions are averaged across species and corrected for $\delta^{13}C$ of atmospheric CO_2, physiological fractionations, altitude, and latitude. Most data plot at MAP ≤800 mm/yr, i.e., relatively dry environments, although wetter environments are also represented. *b*1 = Bibi (51); *b*2 = Bocherens and Drucker (63); *c*1 = Chritz et al. (30); *c*2, *c*3 = Coltrain et al. (32, 20–25 ka and 12 ka); *c*4 = Cerling et al. (2); *d* = DeSantis and Wallace (26); *e* = Eberle et al. (21); *f*1, *f*2 = Fox-Dobbs et al. (31, caribou, equid); *f*3 = France et al. (64); *i* = Iacumin et al. (65); *k* = Koch et al. (19); *m*1 = Morgan et al. (18 at 15.5 Ma); *m*2 = Merceron et al. (52); *m*3 = MacFadden and Higgins (20); *n* = Nelson (66); *p*1 = Passey et al. (49); *p*2 = Palmqvist et al. (27); *s*1 = Ségalen and Lee-Thorp (67); *s*2 = Secord et al. (25); *t*1 = Tütken et al. (68); *t*2 = Tütken et al. (69); *v* = van Dam and Reichart (34); *w* = Wang et al. (29); *z* = Zanazzi and Kohn (33).

maxima. Last, it has been argued that higher past pCO_2 resulted in lower $\delta^{13}C$ values for C3 plants, with a dependence of approximately 2‰/100 ppm (e.g., 39). Eocene pCO_2 estimates of 1,000–1,500 ppm (40), $\delta^{13}C_{atm}$ of −5.5 to −6 (41) and fossil tooth enamel $\delta^{13}C$ (19, 21, 25, 33) would then imply $\delta^{13}C_{diet,meq}$ of −5 to −10‰. Such high values exceed the range of even C4 plants today (e.g., 11, 42), further supporting a negligible pCO_2 correction (43).

Conclusions

Carbon isotope compositions show a distinct but nonlinear increase in $\delta^{13}C$ values with decreasing MAP. A regressed expression provides a new basis for estimating MAP from carbon isotope compositions of fossil tooth enamel or collagen, after first correcting for changes to $\delta^{13}C_{atm}$, altitude, latitude, and physiological fractionations. Research bias toward dry ecosystems appears in analysis of paleoecologies. A downward revision in modern $\delta^{13}C_{ave}$ for C3 plants may improve models of carbon fluxes and soil $\delta^{13}C$ values.

Methods

Data and methods are described in further detail in *SI Text*. In brief, data were taken from the literature, preferring large natural datasets that included date of collection, location, MAP, and mean annual temperature. In some instances, specific locations were not provided, and an estimated or average location was assigned based on descriptions in the primary source. Compositions were corrected for secular changes to the composition of atmospheric CO_2 ($\delta^{13}C_{atm}$) to a common $\delta^{13}C_{atm}$ of −8.00‰ based on modern secular trends (0.023‰/yr; 44). If not reported, the date of collection was assumed to be 2 yr prior to the date of publication. Nearly all climate data were taken directly from the original publications, and any gaps in climate data were obtained from online and published local meteorological tabulations, or, in the few instances where local data were unavailable, from models. Most data are for whole leaves, and for nonleaf data, isotopic offsets were applied as recommended by the authors. Where no recommendation was made, offsets of −2‰ and −0.5‰ were assumed for soil organic matter and leaf litter, respectively (15, 45). It may be argued that environmental parameters other than MAP correlate better with leaf $\delta^{13}C$, such as potential evapotranspiration, water deficit, or growing season precipitation. Although such parameters may be calculated in modern settings, they involve additional variables (e.g., seasonal temperature or precipitation) that may be difficult to constrain in paleoenvironments. Modern data show sufficiently strong correlations with MAP to allow MAP inferences.

Prior to regressions, data were averaged over all C3 plant species at an individual site. This averaging approach differs markedly from all other studies except Stewart et al. (4), whose dataset was over 40 times smaller. Assignment of sites was based on how authors reported their data, i.e., if authors distinguished one set of analyses from another then they were treated as separate sites. Understory, midlevel canopy, and upper-level canopy compositions were distinguished in tropical forests, and analyses from different years were considered as different sites. The total dataset has approximately 570 sites (~95 usable sites from ref. 8) and is especially dense at low MAP (Fig. 1*C*). Many different regression approaches were tested to relate carbon isotope composition to MAP. Averaging data over small MAP ranges (e.g., <100, 100–200, 250–300 mm/yr, etc.) resulted in the highest correlation coefficients (c. 0.95), but this approach is compromised by requiring a priori corrections for altitude and latitude. Instead, the preferred and simpler approach involved regressing $\delta^{13}C$ vs. altitude, latitude, and $\log_{10}(MAP + m_o)$, where m_o is an offset that is determined iteratively and ensures that the intercept of the regression is finite. An alternative regression with Δ as the dependent variable was also calculated. Outliers at $\pm 3\sigma$ from local means were removed iteratively and represent approximately 4% of sites. Understory compositions from dense forests were also omitted (~2% of sites). Data from Schulze et al. (35) for MAP = 130–250 mm/yr deviate significantly from global data trends. These data represent >50% of data in that precipitation range and were collected in a single month during a wet year. To avoid bias compared to other datasets, the Schulze et al. data for <200 and for 200–250 mm/yr were averaged to separate values.

Global distributions of precipitation between 60°S and 75°N latitudes were estimated from 2.5° grids obtained from the Global Precipitation Climatology Center (GPCC) and averaged over 20 yr (1986 to 2005) (http://gpcc.dwd.de). Global plant biomass was either assumed to increase linearly with precipitation or taken from compilations of C3 plant biomass vs. latitude (46), with precipitation vs. latitude for vegetated areas determined from GPCC. The global average C3 value was then predicted by using the fitted curve to model $\delta^{13}C$ vs. MAP, ignoring low $\delta^{13}C$ understory, which represents a negligible fraction of total leaf biomass in the tropics (47, 48). Both methods give comparable results (−28.4 vs. −28.5‰, respectively). Note that these calculations ignore corrections for altitude but include a latitude correction of approximately −0.3‰.

For comparison to herbivore tooth enamel and collagen compositions, correction for changes to $\delta^{13}C_{atm}$ over geologic time was made based on the $\delta^{13}C$ of benthic foraminifera as adjusted for calcification temperature (41; see also refs. 25 and 49). No dependence of plant $\delta^{13}C$ on atmospheric CO_2 concentrations was considered because experimental data show no consistent resolvable relationship for pCO_2 between 200 and 1,300 ppm (43). The effect of this assumption is further discussed. Compositions of fossil teeth and collagen were converted to paleodietary plant composition by subtracting 14‰ (42) and 5‰ (50), respectively, except for three studies that focused exclusively on tooth enamel from bovids younger than 10 Ma (30, 51, 52); for these a larger tooth-diet offset of 14.5‰ was used (53). All paleodiet compositions were converted to Δ, and modern equivalent compositions ($\delta^{13}C_{diet,meq}$) were calculated for $\delta^{13}C_{atm} = -8.00$‰.

ACKNOWLEDGMENTS. The editors and reviewers are thanked for helpful comments. Funded by National Science Foundation Grant EAR0819837.

1. Jacobs BF, Kingston JD, Jacobs LL (1999) The origin of grass-dominated ecosystems. *Ann Mo Bot Gard* 86:590–643.
2. Cerling TE, et al. (1997) Global vegetation change through the Miocene/Pliocene boundary. *Nature* 389:153–158.
3. Farquhar GD, Ehleringer JR, Hubick KT (1989) Carbon isotope discrimination and photosynthesis. *Annu Rev Plant Phys* 40:503–537.
4. Stewart GR, Turnbull MH, Schmidt S, Erskine PD (1995) ^{13}C natural abundance in plant communities along a rainfall gradient: A biological integrator of water availability. *Aust J Plant Physiol* 22:51–55.
5. Schulze E-D, Ellis R, Schulze W, Trimborn P, Ziegler H (1996) Diversity, metabolic types and $\delta^{13}C$ carbon isotope ratios in the grass flora of Namibia in relation to growth form, precipitation and habitat conditions. *Oecologia* 106:352–369.
6. Guo G, Xie G (2006) The relationship between plant stable carbon isotope composition, precipitation and satellite data, Tibet Plateau, China. *Quatern Int* 144:68–71.
7. Keeling CD, Piper SC, Heimann M (1989) A three-dimensional model of atmospheric CO_2 transport based on observed winds: 4. Mean annual gradients and interannual variations. *Aspects of Climate Variability in the Pacific and Western Americas*, ed D Peterson (Am Geophysical Union, Washington, DC), 55, pp 305–363.

8. Diefendorf AF, Mueller KE, Wing SL, Koch PL, Freeman KH (2010) Global patterns in leaf ^{13}C discrimination and implications for studies of past and future climate. *Proc Natl Acad Sci USA* 107:5738–5743.
9. Ehleringer JR, Rundel PW, Palma B, Mooney HA (1998) Carbon isotope ratios of Atacama Desert plants reflect hyperaridity of region in northern Chile. *Rev Chil Hist Nat* 71:79–86.
10. DeLucia EH, Schlesinger WH (1991) Resource-use efficiency and drought tolerance in adjcent Great Basin and Sierran plants. *Ecology* 72:51–58.
11. O'Leary MH (1988) Carbon isotopes in photosynthesis. *Bioscience* 38:328–336.
12. Körner C, Farquhar GD, Roksandic Z (1988) A global survey of carbon isotope discrimination in plants from high altitude. *Oecologia* 74:623–632.
13. Koch PL (1998) Isotopic reconstruction of past continental environments. *Annu Rev Earth Pl Sc* 26:573–613.
14. MacFadden BJ (2000) Cenozoic mammalian herbivores from the Americas: Reconstructing ancient diets and terrestrial communities. *Annu Rev Ecol Sys* 31:33–59.
15. Dawson TE, Mambelli S, Plamboeck AH, Templer PH, Tu KP (2002) Stable isotopes in plant ecology. *Annu Rev Ecol Sys* 33:507–559.
16. Fung I, et al. (1997) Carbon 13 exchanges between the atmosphere and biosphere. *Global Biogeochem Cy* 11:507–533.
17. Wynn JG, Bird MI (2008) Environmental controls on the stable carbon isotopic composition of soil organic carbon: Implications for modelling the distribution of C3 and C4 plants, Australia. *Tellus* 60B:604–621.
18. Morgan ME, Kingston JD, Marino BD (1994) Carbon isotopic evidence for the emergence of C4 plants in the Neogene from Pakistan and Kenya. *Nature* 367(6459): 162–165.
19. Koch PL, Zachos JC, Dettman DL (1995) Stable isotope stratigraphy and paleoclimatology of the Paleogene Bighorn Basin (Wyoming, USA). *Palaeogeogr Palaeocl* 115:61–89.
20. MacFadden BJ, Higgins P (2004) Ancien ecology of 15-million-year-old browsing mammals within C3 plant communities from Panama. *Oecologia* 140:169–182.
21. Eberle J, Fricke H, Humphrey J (2009) Lower-latitude mammals as year-round residents in Eocene Arctic forests. *Geology* 37:499–502.
22. van Dam JA (2006) Geographic and temporal patterns in the late Neogene (12-3 Ma) aridification of Europe: The use of small mammals as paleoprecipitation proxies. *Palaeogeogr Palaeocl* 238:190–218.
23. Wilf P (2000) Late Paleocene-early Eocene climate changes in southwestern Wyoming: Paleobotanical analysis. *Geol Soc Am Bull* 112:292–307.
24. Terry DOJ (2001) Paleopedology of the Chadron Formation of Northwestern Nebraska: Implications for paleoclimatic change in the North American midcontinent across the Eocene-Oligocene boundary. *Palaeogeogr Palaeocl* 168:1–38.
25. Secord R, Wing SL, Chew A (2008) Stable isotopes in early Eocene mammals as indicators of forest canopy structure and resource partitioning. *Paleobiology* 34:282–300.
26. DeSantis LRG, Wallace SC (2008) Neogene forests from the Appalachians of Tennessee, USA: Geochemical evidence from fossil mammal teeth. *Palaeogeogr Palaeocl* 266:59–68.
27. Palmqvist P, Groecke DR, Arribas A, Farina RA (2003) Paleoecological reconstruction of a lower Pleistocene large mammal community using biogeochemical ($\delta^{13}C$, $\delta^{15}N$, $\delta^{18}O$, Sr:Zn) and ecomorphological approaches. *Paleobiology* 29:205–229.
28. White TD, et al. (2009) Macrovertebrate paleontology and the Pliocene habitat of Ardipithecus ramidus. *Science* 326:87–93.
29. Wang Y, et al. (2008) Stable isotopes in fossil mammals, fish and shells from Kunlun Pass Basin, Tibetan Plateau: paleo-climatic and paleo-elevation implications. *Earth Planet Sc Lett* 270:73–85.
30. Chritz KL, et al. (2009) Palaeobiology of an extinct Ice Age mammal: Stable isotope and cementum analysis of giant deer teeth. *Palaeogeogr Palaeocl* 282:133–144.
31. Fox-Dobbs K, Leonard JA, Koch PL (2008) Pleistocene megafauna from eastern Beringia: Paleoecological and paleoenvironmental interpretations of stable carbon and nitrogen isotope and radiocarbon records. *Palaeogeogr Palaeocl* 261:30–46.
32. Coltrain JB, et al. (2004) Rancho La Brea stable isotope biogeochemistry and its implications for the palaeoecology of late Pleistocene, coastal Southern California. *Palaeogeogr Palaeocl* 205:199–219.
33. Zanazzi A, Kohn MJ (2008) Ecology and physiology of White River mammals based on stable isotope ratios of teeth. *Palaeogeogr Palaeocl* 257:22–37.
34. van Dam JA, Reichart GJ (2009) Oxygen and carbon isotope signatures in late Neogene horse teeth from Spain and application as temperature and seasonality proxies. *Palaeogeogr Palaeocl* 274:64–81.
35. Schulze E-D, Turner NC, Nicolle D, Schumacher J (2006) Leaf and wood carbon isotope ratios, specific leaf areas and wood growth of Eucalyptus species across a rainfall gradient in Australia. *Tree Physiol* 26:479–492.
36. Hartman G, Danin A (2010) Isotopic values of plants in relation to water availability in the Eastern Mediterranean region. *Oecologia* 162:837–852.
37. Shanyengana ES, Henschel JR, Seely MK, Sanderson RD (2002) Exploring fog as a supplementary water source in Namibia. *Atmos Res* 64:251–259.
38. Westbeld A, et al. (2009) Fog deposition to a Tillandsia carpet in the Atacama Desert. *Ann Geophys* 27:3571–3576.
39. Feng X, Epstein S (1995) Carbon isotopes of trees from arid environments and implications for reconstructing atmospheric CO_2 concentration. *Geochim Cosmochim Ac* 59:2599–2608.
40. Pagani M, Zachos JC, Freeman KH, Tipple B, Bohaty S (2005) Marked decline in atmospheric carbon dioxide concentrations during the Paleogene. *Science* 309:600–603.
41. Tipple BJ, Meyers SR, Pagani M (2010) Carbon isotope ratio of Cenozoic CO_2: A comparative evaluation of available geochemical proxies. *Paleoceanogr* 25 10.1029/2009PA001851.
42. Cerling TE, Harris JM (1999) Carbon isotope fractionation between diet and bioapatite in ungulate mammals and implications for ecological and paleoecological studies. *Oecologia* 120:347–363.
43. Arens NC, Jahren AH, Amundson RG Can C3 plants faithfully record the carbon isotopic composition of atmospheric carbon dioxide? *Paleobiology* 26:137–164.
44. Keeling CD, et al. (2001) Exchanges of atmospheric CO_2 and $^{13}CO_2$ with the terrestrial biosphere and oceans from 1978 to 2000. I. Global aspects. *SIO Reference No. 01-06* pp 1–28.
45. Bowling DR, Pataki DE, Randerson JT (2008) Carbon isotopes in terrestrial ecosystem pools and CO_2 fluxes. *New Phytol* 178:24–40.
46. Still CJ, Berry JA, Collatz GJ, DeFries RS (2003) Global distribution of C3 and C4 vegetation: Carbon cycle implications. *Global Biogeochem Cy* 17 10.1029/2001GB001807.
47. Medina E, Minchin P (1980) Stratification of $\delta^{13}C$ values of leaves in Amazonian rain forests. *Oecologia* 45:377–378.
48. Cerling TE, Hart JA, Hart TB (2004) Stable isotope ecology in the Ituri Forest. *Oecologia* 138:5–12.
49. Passey BH, et al. (2002) Environmental change in the Great Plains; an isotopic record from fossil horses. *J Geol* 110:123–140.
50. Ambrose SH, DeNiro MJ (1986) The isotopic ecology of East African mammals. *Oecologia* 69:395–406.
51. Bibi F (2007) Dietary niche partitioning among fossil bovids in late Miocene C3 habitats: Consilience of functional morphology and stable isotope analysis. *Palaeogeogr Palaeocl* 253:529–538.
52. Merceron G, Zazzo A, Spassov N, Geraads D, Kovachev D (2006) Bovid paleoecology and paleoenvironments from the Late Miocene of Bulgaria: evidence from dental microwear and stable isotopes. *Palaeogeogr Palaeocl* 241:637–654.
53. Passey BH, et al. (2005) Carbon isotope fractionation between diet, breath CO_2, and bioapatite in different mammals. *J Archaeol Sci* 32:1459–1470.
54. Gouveia AC, Freitas H (2009) Modulation of leaf attributes and water use efficiency in *Quercus suber* along a rainfall gradient. *Trees* 23:267–275.
55. Hatté C, et al. (2001) $\delta^{13}C$ of loess organic matter as a potential proxy for paleoprecipitation. *Quaternary Res* 55:33–38.
56. Leffler AJ, Enquist BJ (2002) Carbon isotope composition of tree leaves from Guanacaste, Costa Rica: Comparison across tropical forests and tree life history. *J Trop Ecol* 18:151–159.
57. Liu W, et al. (2005) $\delta^{13}C$ variation of C3 and C4 plants across an Asian monsoon rainfall gradient in arid northwestern China. *Glob Change Biol* 11:1094–1100.
58. Miller JM, Williams RJ, Farquhar GD (2001) Carbon isotope discrimination by a sequence of Eucalyptus species along a subcontinental rainfall gradient in Australia. *Funct Ecol* 15:222–232.
59. Macfarlane C, Adams MA, White DA (2004) Productivity, carbon isotope discrimination an leaf traits of trees of Eucalyptus globulus Labill in relation to water availability. *Plant Cell Environ* 27:1515–1524.
60. Roden JS, Bowling DR, McDowell NG, Bond BJ, Ehleringer JR (2005) Carbon and oxygen isotope ratios of tree ring cellulose along a precipitation transect in Oregon, United States. *J Geophys Res* 110 10.1029/2005JG000033.
61. Song M, et al. (2008) Leaf $\delta^{13}C$ reflects ecosystem patterns and responses of alpine plants to the environments on the Tibetan Plateau. *Ecography* 31:499–508.
62. Youfeng N, Weiguo L, Zhisheng A (2008) A 130-ka reconstruction of precipitation on the Chinese Loess Plateau from organic carbon isotopes. *Palaeogeogr Palaeocl* 270:59–63.
63. Bocherens H, Drucker D (2003) Trophic level isotopic enrichment of carbon and nitrogen in bone collagen: Case studies from Recent and ancient terrestrial ecosystems. *Int J Osteoarcheol* 13:46–53.
64. France CAM, Zelanko PM, Kaufman AJ, Holtz TR (2007) Carbon and nitrogen isotopic analysis of Pleistocene mammals from the Saltville Quarry (Virginia, USA): Implications for trophic relationships. *Palaeogeogr Palaeocl* 249:271–282.
65. Iacumin P, Bocherens H, Delgado Huertas A, Mariotti A, Longinelli A (1997) A stable isotope study of fossil mammal remains from the Paglicci Cave, southern Italy: N and C as palaeoenvironmental indicators. *Earth Planet Sc Lett* 148:349–357.
66. Nelson SV (2007) Isotopic reconstructions of habitat change surrounding the extinction of Sivapithecus, a Miocene hominoid, in the Siwalik Group of Pakistan. *Palaeogeogr Palaeocl* 243:204–222.
67. Ségalen L, Lee-Thorp JA (2009) Palaeoecology of late Early Miocene fauna in the Namib based on $^{13}C/^{12}C$ and $^{18}O/^{16}O$ ratios of tooth enamel and ratite eggshell carbonate. *Palaeogeogr Palaeocl* 277:191–198.
68. Tütken T, Vennemann TW, Janz H, Heizmann EPJ (2006) Palaeoenvironment and palaeoclimate of the Middle Miocene lake in the Steinheim basin, SW Germany: A reconstruction from C, O, and Sr isotopes of fossil remains. *Palaeogeogr Palaeocl* 241:457–491.
69. Tütken T, Vennemann T (2009) Stable isotope ecology of Miocene large mammals from Sandelzhausen, southern Germany. *Palaeont Z* 83:207–226.